GRAPHENES

Edge-Modified Zigzag Graphene Nanoribbons: Structure and Electronic Properties

V. A. Soroko[a], *, K. G. Batrakov[a], and L. A. Chernozatonskii[b]

*[a] Research Institute for Nuclear Problems, Belarusian State University,
ul Bobruiskaya 11, Minsk, 220030 Belarus*
* e-mail: 40.ovasil@gmail.com
*[b] Emanuel Institute of Biochemical Physics, Russian Academy of Sciences,
ul. Kosygina 4, Moscow, 119334 Russia*
Received April 15, 2014

Abstract—Control of the band gap of graphene nanoribbons is an important problem for the fabrication of effective radiation detectors and transducers operating in different frequency ranges. The periodic edge-modified zigzag graphene nanoribbon (GNR) provides two additional parameters for controlling the band gap of these structures, i.e., two GNR arms. The dependence of the band gap E_g on these parameters is investigated using the π-electron tight-binding method. For the considered nanoribbons, oscillations of the band gap E_g as a function of the nanoribbon width are observed not only in the case of armchair-edge graphene nanoribbons (as for conventional graphene nanoribbons) but also for zigzag GNR edges. It is shown that the change in the band gap E_g due to the variation in the length of one GNR arm is several times smaller than that due to the variation in the nanoribbon width, which provides the possibility for a smooth evolution of the band gap in the energy spectrum of the considered graphene nanoribbons.

1. INTRODUCTION

Graphene nanoribbons (GNRs) are quasi-one-dimensional carbon structures that can be obtained by "cutting" a graphene sheet into strips of nanometer width [1]. As a theoretical model for the study of edge properties of graphite, these structures were considered in [2]. Since the preparation of graphene in a free-standing state [3], such objects have been actively studied both theoretically [4–8] and experimentally [9–11]. In parallel to the aforementioned studies, methods of their synthesis have been developed rapidly [1, 11–12]. Following the simplest single-layer ribbons, two-layer systems have been investigated [14–16], and the influence of stacking of layers on their properties has been analyzed [17]. Investigations have also been undertaken into the influence of an electric field [18], mechanical stresses [19], edge defects [20], and disordering of the nanoribbon edge [6, 21] on the properties of such systems. A number of GNR-based superlattices [22–24] and "tracks" on a graphene sheet [25–27] have been considered. The development of the method for synthesizing graphene nanoribbons, which made it possible, through self-assembly, to obtain armchair graphene nanoribbons with atomically smooth edges, as well as nanoribbons with a more complex edge shape [13], has stimulated further investigation of systems similar to superlattices [28, 29].

In this work, we have studied edge-modified zigzag graphene nanoribbons (ZGNRs). We have considered structures that differ from the structures studied in [24] by the asymmetry with respect to the longitudinal nanoribbon axis and from those examined in [28, 29] by the apex angle. We have developed a method for describing edge-modified ZGNRs within the formalism for carbon nanotubes (CNTs), which allows consideration of the structures that are asymmetric with respect to the transverse axis lying in the nanoribbon plane and do not fit into the framework of the models discussed in [28, 29]. On this basis, we have revealed new interesting features in the behavior of the band gap in the energy spectra of edge-modified ZGNRs.

2. CRYSTAL STRUCTURE AND CLASSIFICATION

Below, we consider periodic edge-modified zigzag graphene nanoribbons (Fig. 1). A distinctive feature of these structures is the presence of the following elements: two arms ($\mathbf{L}_1$ and $\mathbf{L}_2$), i.e., straight-line segments, with the apex angle φ between them. In the considered structures, one edge can be obtained by a simple translation of the other edge by a vector $\mathbf{W}$ whose magnitude determines the "width" of the edge-modified ZGNR (see Fig. 1). Therefore, any edge-modified ZGNR can be described by a set of vectors $\mathbf{L}_1$, $\mathbf{L}_2$, and $\mathbf{W}$. Since each of them is the vector of the crystal lattice of graphene, they can be expressed in terms of the vectors $\mathbf{a}_1$ and $\mathbf{a}_2$ of the graphene unit cell.
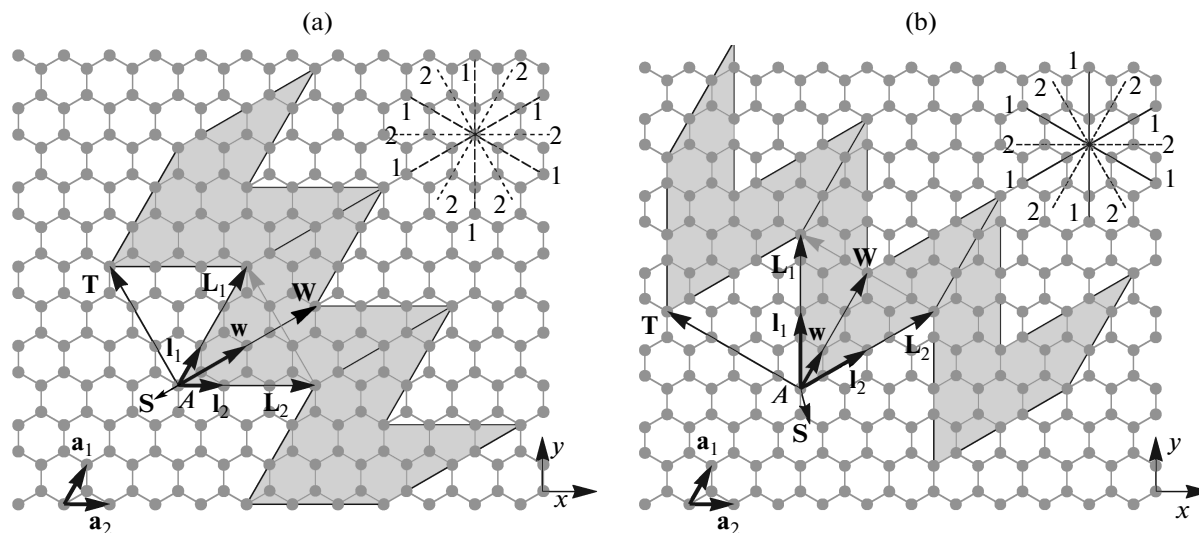
Fig. 1. Structures of the graphene nanoribbons with periodically jagged edges and the vectors $\mathbf{L}_1$, $\mathbf{L}_2$, and $\mathbf{W}$ (the corresponding elementary vectors $\mathbf{I}_1$, $\mathbf{I}_2$, and $\mathbf{w}$) characterizing these structures, $\mathbf{T}$ is the translation period of the unit cell of the edge-modified GNR, and A is the carbon atom of the A sublattice of the graphene (the carbon atom of the B sublattice is located at the origin of the coordinates): (a) edge-modified zigzag GNR (compare with Fig. 2a) and (b) edge-modified armchair GNR (compare with Fig. 2c). Shown in the lower left corner are the basis vectors of the unit cell of the graphene hexagonal lattice $\mathbf{a}_1$ and $\mathbf{a}_2$. After the parallel translation by the vector $\mathbf{S}$, the gray area covers all carbon atoms of the graphene lattice, which enter into the composition of the edge-modified GNR.

The arbitrary vector of the crystal lattice of graphene $\mathbf{V}$ can be represented in the form

$$\mathbf{V} = n\mathbf{a}_1 + m\mathbf{a}_2. \qquad (1)$$

Among all the possible directions of the vector $\mathbf{V}$, there are directions along which, after the cutting of the graphene sheet, we obtain armchair (A) or zigzag (Z) edges, i.e., lines 1−1 and 2−2 in Fig. 1, respectively. For these directions, the vector $\mathbf{V}$ can be written as

$$\mathbf{V} = \nu\mathbf{v}, \qquad (2)$$

where $\mathbf{v}$ is the vector of the unit translation along this direction and ν is an integer. Considering the vectors $\mathbf{L}_1$, $\mathbf{L}_2$, and $\mathbf{W}$, we restrict ourselves to their directions Z and A. Then, for each of them, we can introduce the elementary vector (see Fig. 1). Hence, the magnitude of the vector can be expressed in terms of an integer index. For a given subset of elementary vectors $\mathbf{I}_1$, $\mathbf{I}_2$, and $\mathbf{w}$, there can be a set of subsets of indices (l_1, l_2, w),

each corresponding to a specific set of vectors $\mathbf{L}_1$, $\mathbf{L}_2$, and $\mathbf{W}$. Therefore, we can say that a set of elementary vectors $\mathbf{I}_1$, $\mathbf{I}_2$, and $\mathbf{w}$ specifies the type of ribbons and a set of integer indices defines a particular ribbon within the specified type. The structures characterized by different sets of elementary vectors, in essence, differ only in the arm edge type and in the value of the apex angle φ, which can also be defined as the angle between the vectors $\mathbf{I}_1$ and $\mathbf{I}_2$. We restrict ourselves to edge-modified ZGNRs of four types (T φ), where T takes on values "Z" or "A" for the cases of ribbons with zigzag or armchair arms, respectively, and φ corresponds to the apex angle $\varphi = 60°$ or $120°$ (Fig. 2). Other types of ribbons with $\varphi = 30°$, $90°$, and $150°$, if we follow the directions Z and A for the vectors $\mathbf{I}_1$ and $\mathbf{I}_2$, as well as ribbons with other values of φ upon deviation from these directions, can be considered similarly. The table presents the coordinates of the elementary vectors $\mathbf{I}_1$, $\mathbf{I}_2$, and $\mathbf{w}$ in the basis of vectors $\mathbf{a}_1$ and $\mathbf{a}_2$ for each of the four types of edge-modified ZGNRs. The considered structures are also characterized by the following two features: the vector of width $\mathbf{W}$ is the bisector of the apex angle φ, and one edge of the unit cell of the superlattice of the edge-modified ZGNR, which is translated by the vector $\mathbf{W}$, coincides with its other edge.

The period of translation $\mathbf{T}$ of the unit cell of the edge-modified ZGNR can be expressed in terms of the introduced quantities as follows:

$$\mathbf{T} = \mathbf{L}_1 - \mathbf{L}_2 = l_1\mathbf{I}_1 - l_2\mathbf{I}_2, \qquad (3)$$

Coordinates of the elementary vectors characterizing different types of edge-modified ZGNRs

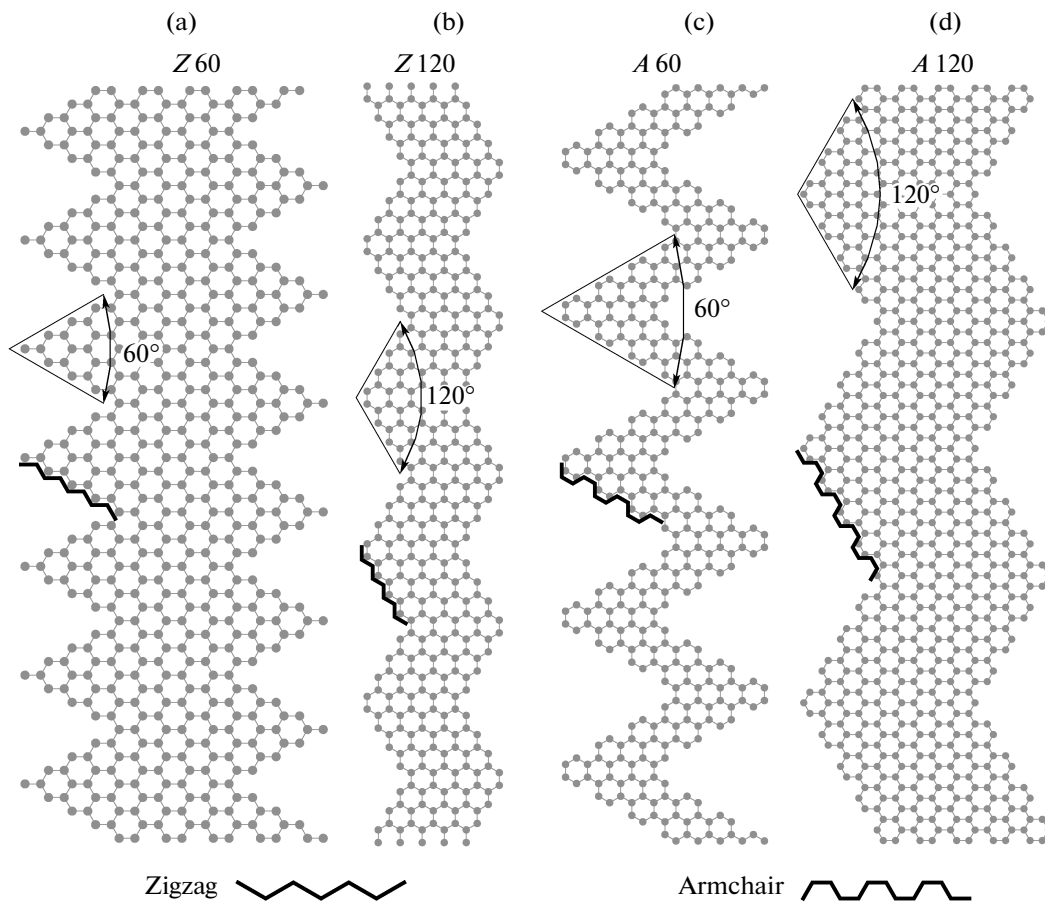| Elementary vectors	Z60	Z120	A60	A120
$\mathbf{I}_1$	(1, 0)	(1, −1)	(2, −1)	(2, −1)
$\mathbf{I}_2$	(0, 1)	(0, 1)	(1, 1)	(−1, 2)
$\mathbf{w}$	(1, 1)	(1, 0)	(1, 0)	(1, 1)

Fig. 2. Four types of edge-modified GNRs with different types of arms and angles φ: (a) Z60, (b) Z120, (c) A60, and (d) A120.
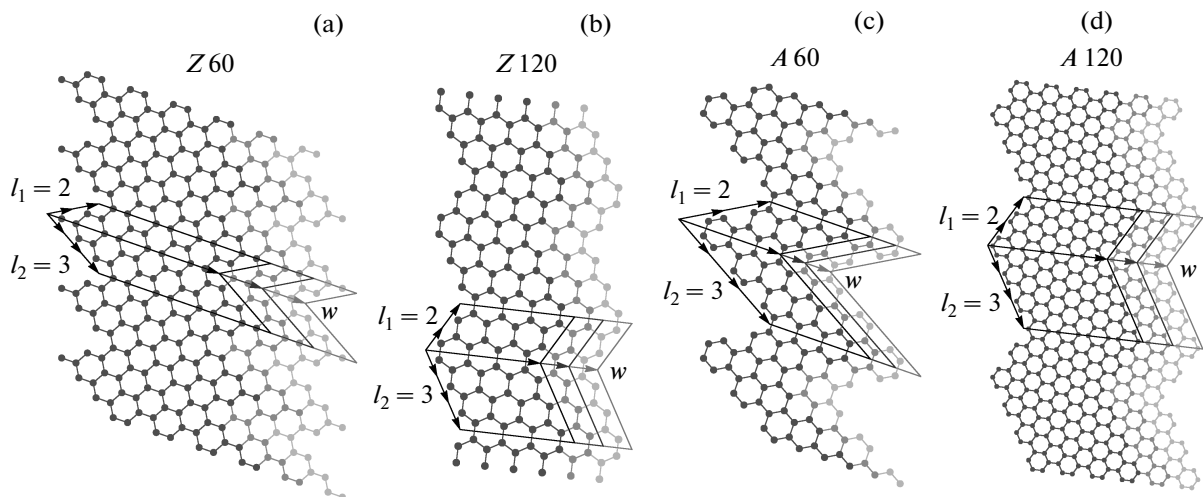

Fig. 3. Increase in the width of the edge-modified GNRs: (a) Z60, (b) Z120, (c) A60, and (d) A120.

and the number of atoms in the unit cell is given by the formula

$$N = \lambda(l_1 + l_2)w, \qquad (4)$$

where $\lambda = 2$ in the case of the nanoribbons Z60, Z120, and A60 and $\lambda = 6$ in the case of the nanoribbon A120. The difference in the values of λ for different types of nanoribbons is associated with the fact that an increase
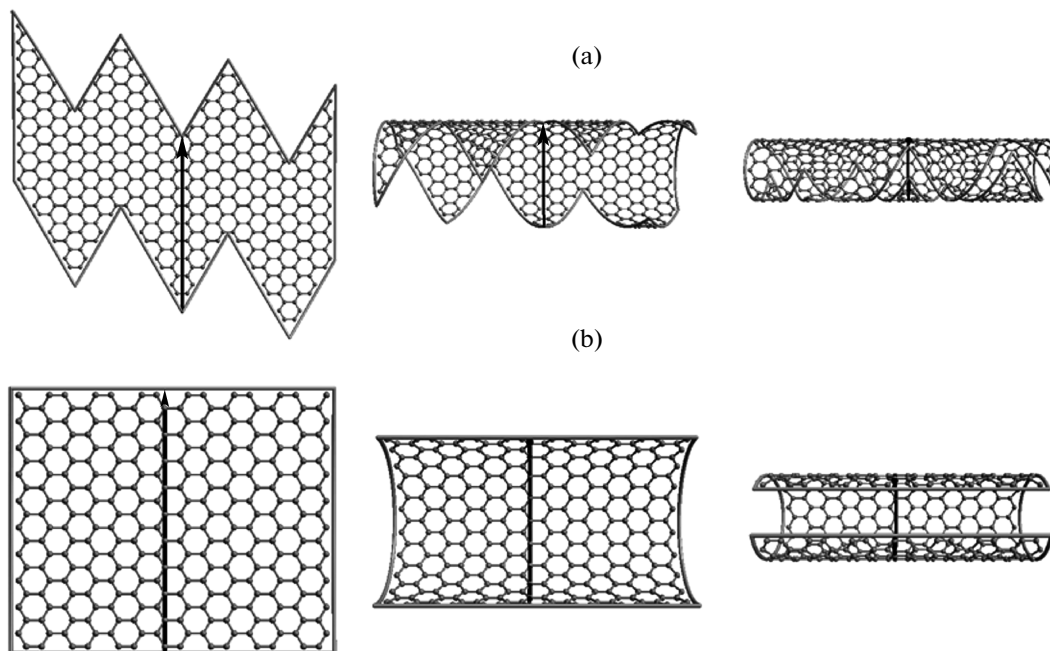
Fig. 4. Folding of (a) edge-modified GNR A60 (*4*, *3*, *10*) and (b) conventional armchair graphene nanoribbon in the CNT(10,0). The vector in the figure is the vector of width **W** of the edge-modified GNR (the vector of width of the GNR and chirality of the corresponding CNT). Similarly, this figure can be interpreted as the zigzag and straight (for GNR) cutting of the CNT.

in the nanoribbon width by unity (i.e., index *w*) corresponds to the addition of a chain of dimers consisting of atoms belonging to different graphene sublattices *A* and *B* in the first case and to the addition of a chain of hexagons the second case (see Fig. 3).

3. RELATION TO OTHER CARBON NANOSTRUCTURES

Before investigating the electronic properties of the edge-modified ZGNRs, we establish their relation to another class of carbon nanostructures, namely, carbon nanotubes. As can be seen, the edge-modified ZGNRs considered above can be rolled into cylinders, which are nothing else than nanotubes. The opposite is also true: an edge-modified ZGNR, like the conventional GNRs [12], can be obtained by cutting any CNT. In our case (see Fig. 4), it can be a zigzag or armchair nanotube. Of course, unlike the case of conventional GNRs, in the case of edge-modified ZGNRs, the CNT should be cut along a broken zigzag line (not to be confused with the zigzag edge), which is formed by the vectors **L**$_1$ and **L**$_2$ and, upon rotation of the nanotube, transforms into edges of the considered nanoribbons. For edge-modified ZGNRs of any type, there is a simple relation between the chirality vector **C** of the CNT [30] and the vector of width **W** of the edge-modified ZGNR: **W** = **C**. Using formulas (1) and (2),

we can easily obtain the relationship for the edge-modified ZGNRs

$$\mathbf{W} = w\mathbf{w} = \mathbf{C} = n\mathbf{a}_1 + m\mathbf{a}_2$$

$$= \frac{n\mathbf{a}_1 + 0\mathbf{a}_2, \ zigzag}{n\mathbf{a}_1 + n\mathbf{a}_2, \ amchair} = \frac{n(\mathbf{a}_1 + 0\mathbf{a}_2)}{n(\mathbf{a}_1 + \mathbf{a}_2)},$$

from which it follows that $n = w$, where n is the index characterizing the zigzag or armchair CNTs [30].

4. METHOD OF INVESTIGATION

The electronic properties of edge-modified ZGNRs were investigated using the π-electron tight-binding method [30, 31]. This method is simple and economical in respect of the required computational power and, hence, time. Furthermore, this method adequately reproduces the character of the band spectra of the considered carbon nanostructures [1]. Under this method, the energy bands are obtained by solving the problem of the eigenvalues of the Hamiltonian matrix. The dimension of this matrix is equal to σ × σ, where σ is the number of carbon atoms in the unit cell of the nanoribbon. If the atoms in the unit cell are numbered, each element of the Hamiltonian matrix H_{ij} has the form

$$H_{ij} = \sum_{p=1}^{n} t_{ij0} \exp(i\mathbf{k}\mathbf{r}_{ijp}) \vartheta(\Delta - |r_{ij0} - r_{ijp}|), \quad (7)$$

where t_{ij0} is the hopping integral between the ith and jth atoms (for the nearest neighbors, this integral was chosen to be 3.12 eV [31]) separated by the distance r_{ij0}, r_{ij1} is the distance between ith and jth atoms in the given unit cell, r_{ijp} is the distance between the ith atom in the given unit cell and the jth atom of one of the adjacent unit cells ($p \neq 1$), $\mathbf{k}$ is the electron quasi-wave vector, $\mathbf{r}_{ijp}$ is the vector connecting positions of the ith atom (the beginning of the vector) and the jth atom (the end of the vector), and φ is the Heaviside function. As can be seen from formula (7), if the distance between the ith and jth atoms (r_{ijp}) differs from the distance between these atoms in the ideal graphene lattice (r_{ij0}) by more than Δ (for a better understanding, we should imagine the edge-modified ZGNR built into the graphene lattice as in Fig. 1; in this case, the graphene plays the role of a reference system), the bond between these atoms is ignored. Hence, the parameter Δ can be called the sensitivity of the algorithm used. Actually, for large values of Δ, the corresponding hopping integral should also change: its value should increase with a decrease in the C–C bond length and, on the contrary, it should decrease as the C–C bond length increases. These deformations occur at the edge of the nanoribbon and can be taken into account by generalizing formula (7) as follows [32]:

$$H_{ij} = \sum_{p=1}^{n} t_{ij} \exp(i\mathbf{k}\mathbf{r}_{ijp})\vartheta(\Delta - |r_{ij0} - r_{ijp}|), \quad (8)$$

where t_{ij} is the hopping integral, which depends on the distance between the atoms. In formula (8), the dependence of the hopping integral on the distance is described by formula (2) from [32]

$$t_{ij} = t_{ij0}\exp\left(\beta\frac{r_{ij0} - r_{ijp}}{r_{ij0}}\right),$$

where $\beta = 3$ is the parameter determining the rate of decrease in the hopping integral with increasing distance between the atoms.

The matrix filling algorithm corresponding to formula (8) was tested by filling the matrix for GNRs [5], CNTs [33], graphene and bigraphene [31]. The results of calculations for these nanostructures demonstrated an excellent agreement with the results of the aforementioned studies and reproduce such features of band structures as the cone for graphene, the trigonal structure of bands near the K point when taking into account the hopping integrals between the A–A and A–B atoms in adjacent layers for bigraphene, doubly degenerate levels for CNTs, and special states at zigzag edges for GNRs [2].

The electronic band structures were calculated for optimized geometries of the edge-modified ZGNRs. The nanoribbon edges were passivated by hydrogen atoms; then, the geometry of the structure was optimized using the Large-Scale Atomic/Molecular Massively Parallel Simulator (LAMMPS) package [34]. This package implements the classical molecular dynamics based on specified potentials. The geometry of the system was optimized using the Adaptive Intermolecular Reactive Empirical Bond Order (AIREBO) potential proposed by Stuart et al. [35] for systems consisting of carbon and hydrogen atoms. In the LAMMPS package, this potential is realized in its original formulation [35]. In the geometry optimization, we used the method of the conjugate gradient in the Polak–Ribiére version, which is more effective in comparison with other versions of the conjugate gradient method. This algorithm minimizes not only the potential energy of the system but also the forces acting on individual atoms, so that the changes in the energy would be only negative. In this case, we used the following criteria for the termination of iterations: the relative change in the energy is less than 10^{-4}; all the forces acting on the atoms do not exceed 10^{-6} eV/Å; the change in the position of the atoms is less than the computer accuracy of the calculations; the excess of the maximum number of iterations (15000); and the excess of the maximum number of calculations of energies/forces (30000).

5. THE BAND GAP

Using the methods described above, we investigated the dependences of the band gap E_g on the indices characterizing the edge-modified ZGNRs. First, we considered the dependence of the band gap on the width of nanoribbons for the case where the GNR arms remain unchanged. The obtained results are presented in Figs. 5 and 6. Our attention was drawn to the fact that, for the edge-modified ZGNR Z60, the band gap significantly decreased with an increase in the nanoribbon width. Therefore, we decided to use two types of functions for the approximation of the calculated data: the exponential function and the inverse power function.

It can be seen from Fig. 5 that the exponential function better describes the set of data for the Z60 nanoribbons. In contrast, the dependence of the band gap E_g on the width of the A120 nanoribbon is better described by the inverse power function. It should be noted that the power-law decay of the band gap E_g is also characteristic of the conventional armchair GNR [7, 8, 36]. The exponential decay was mentioned in [37], where the authors investigated, in the most general form, periodic modifications of the zigzag edges of the graphene hexagonal lattice. In that paper, however, the authors restricted their consideration to the so-called minimum edge, where for each carbon atom at the boundary there is one bond passivated by hydrogen. At the same time, because of the presence of an angular atom with two attached hydrogen atoms in the Z60 nanoribbons, they should be assigned to a more general case, where the exponential decay of the band
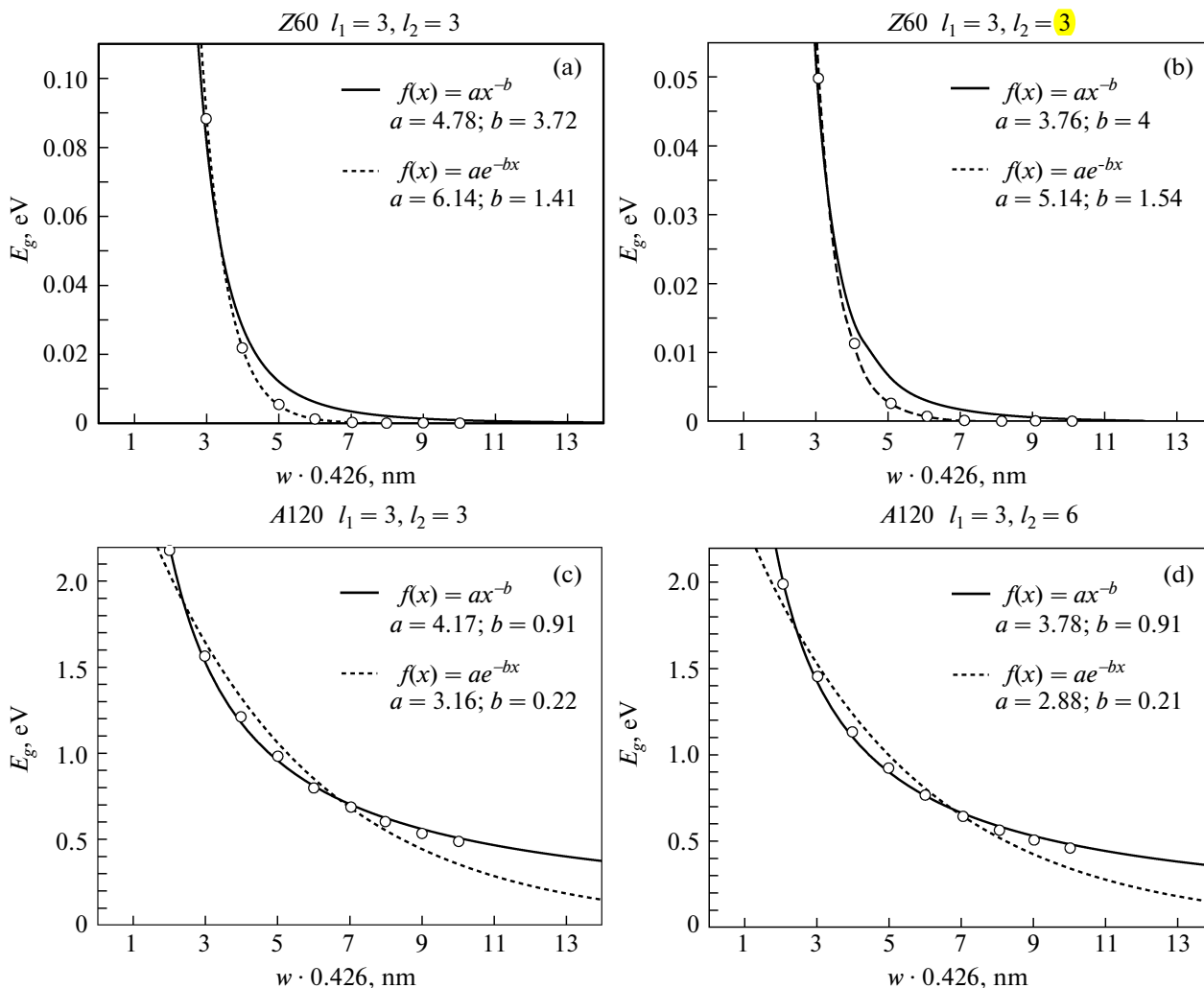
Fig. 5. Dependences of the band gap E_g on the width of the edge-modified GNR: (a) Z60, $l_1 = l_2 = 3$; (b) Z60, $l_1 = 3$, $l_2 = 6$; (c) A120, $l_1 = l_2 = 3$; and (d) A120, $l_1 = 3$, $l_2 = 6$.

gap has still not been confirmed by numerical calculations.

For the nanoribbons Z120 and A60, as can be seen from Fig. 6, there are oscillations of the band gap. The period of these oscillations is multiple of three. Therefore, nanoribbons of this type, as well as the conventional armchair GNRs, can be conditionally divided into three series. Each of these series behaves in accordance with the law of inverse proportionality of the band gap E_g. However, there is a fundamental difference between the oscillations of the band gap E_g for the nanoribbons Z120 and A60. In the first case, the oscillations decay with an increase in the difference between the indices of the GNR arms, as well as with an increase in the indices of both GNR arms, whereas in the second case, for the A60 nanoribbons, the oscillations of the band gap are retained.

This type of oscillations is known for zigzag CNTs (the edge-modified GNRs Z120 and A60 are rolled into such CNTs), armchair GNRs [36], and some other semiconducting graphene nanoribbons [4]. It is of interest that, in [4], the authors observed in GNRs the decay of oscillations of the band gap E_g as a function of the angle of chirality of the original nanotube. In that paper, GNRs were considered as unfolded nanotubes of different chiralities (the folding of an achiral zigzag CNT is shown in Fig. 4b). However, as was noted above, the vector of width of the edge-modified ZGNR corresponds to the chirality vector of the CNT; hence, in our case, the crystallographic orientation of the nanoribbons remained constant. The decay of oscillations of the band gap E_g can be explained as follows. Depending on the ratio between the indices (l_1, l_2, w), all the nanoribbons can be conditionally divided into three groups

(1) $l_1, l_2 < w$.
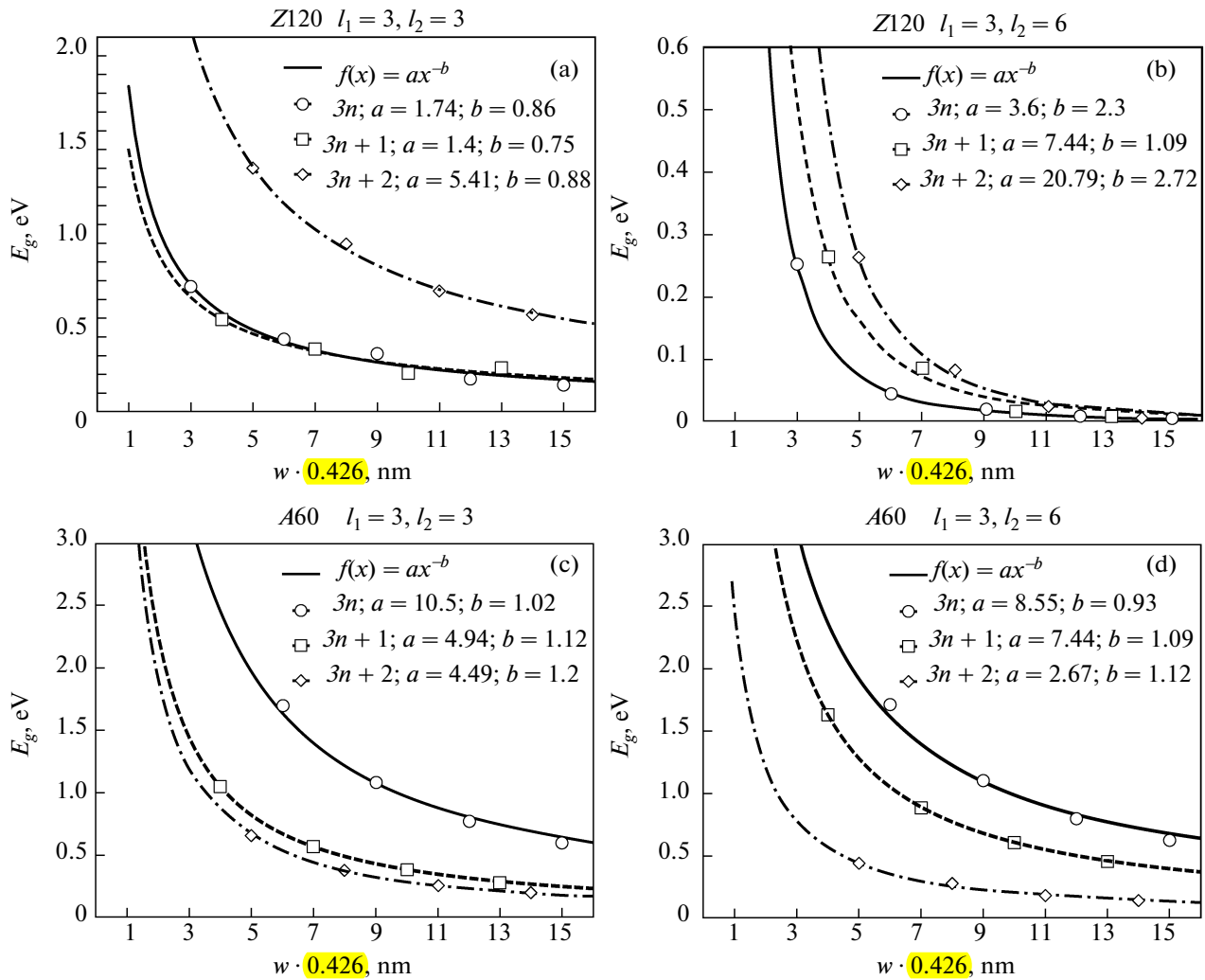
(2) $l_1 (l_2) < w < l_2 (l_1)$.

(3) $w < l_1, l_2$.

Fig. 6. Dependences of the band gap E_g on the width of the edge-modified GNR: (a) Z120, $l_1 = l_2 = 3$; (b) Z120, $l_1 = 3$, $l_2 = 6$; (c) A60, $l_1 = l_2 = 3$; and (d) A60, $l_1 = 3$, $l_2 = 6$.

Nanoribbons of the first group can be represented as GNRs (the armchair GNRs for the nanoribbons Z120 and A60; see the corresponding nanoribbons in Fig. 2) from which the GNRs can be obtained by cutting triangular segments, Nanoribbons of the third group can be represented as a sequence of GNRs connected at particular angles (the zigzag GNRs for the Z120 nanoribbons and the armchair GNRs for the A60 nanoribbons). For large indices of the arms, the influence of junction regions on the band gap E_g becomes negligible, and the band structure of the Z120 nanoribbons tends to the band structure of the zigzag GNR, in which, if the ordering of spins at the edge of the nanoribbon is ignored [2, 36], the band gap is absent. At the same time, the band structure of the A60 nanoribbons tends to the band structure of the armchair GNR, which, as noted above, are characterized by oscillations of the band gap [7, 8]. For small indices of the arms, the behavior of the band gap E_g repro-

duces the behavior of the band gap of the armchair GNR.

It is known that the width of GNRs is a good control parameter for the band gap. According to our calculations, the same is true for edge-modified ZGNRs. This behavior is explained by the localization of charge carriers in one of the directions of the two-dimensional graphene lattice due to the reflection from the edge potential barrier. However, in quantum mechanics, a particle with a certain probability can be reflected not only from the barrier but also on the potential step, which can also be responsible for the localization of charge carriers. In the considered structures, according to their geometry the potential undergoes rotations in the range of apex angles, which represent potential steps. Since the probability of reflection from the step is less than the probability of reflection from the barrier (at the edge of the nanoribbon, the potential barrier is infinite, because the parti-
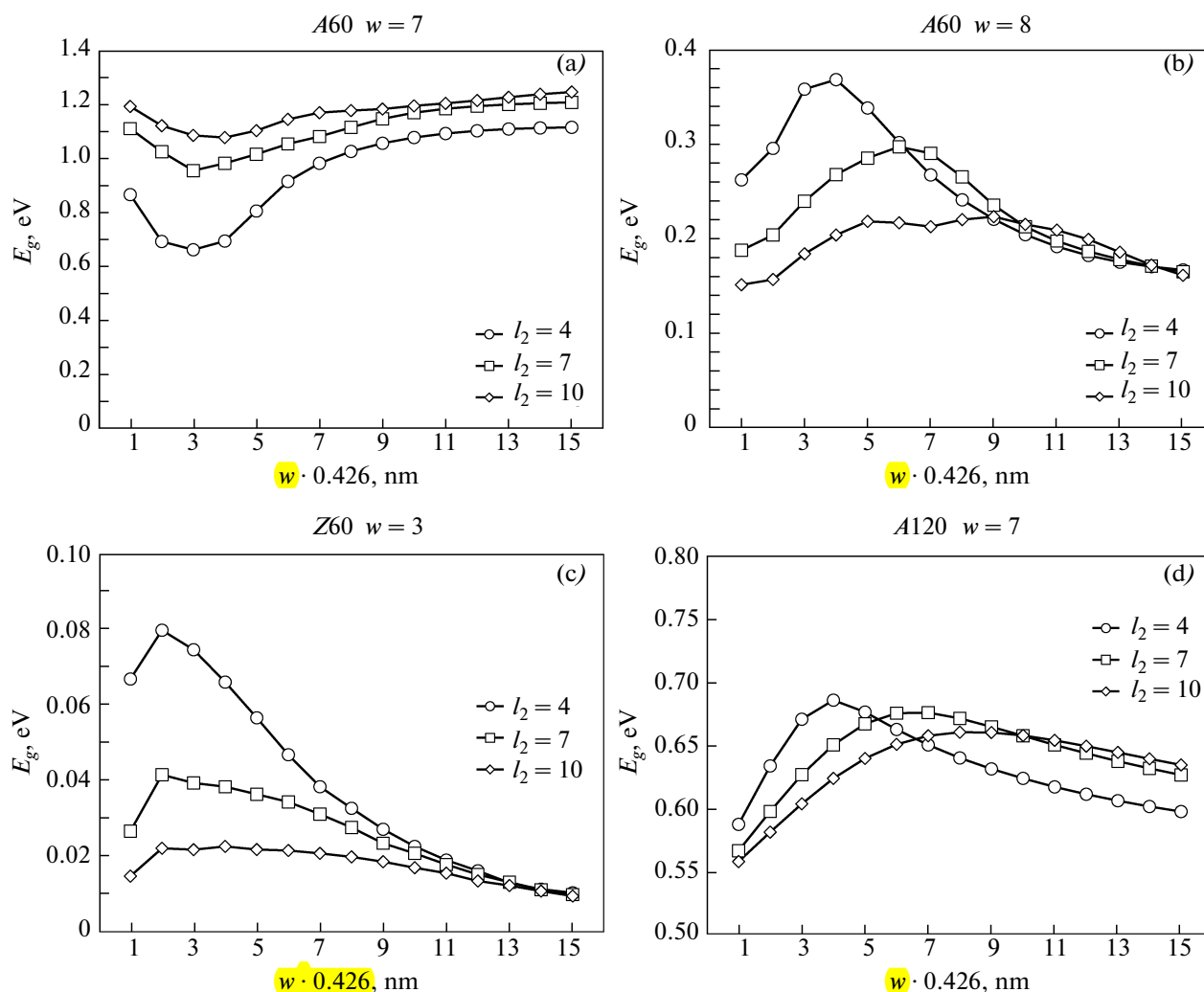
Fig. 7. Dependences of the band gap E_g on the length of the GNR arm l_1 for the nanoribbons A60 ($w = 7, 8$), Z60 ($w = 3$), and A120 ($w = 7$).

cle nowhere tunnel), the localization of charge carriers should be weaker. In other words, changes in the band gap due to variations in the parameters l_1 and l_2 will be less than the changes in the band gap due to variations in the parameter w. This assumption was verified by analyzing the dependence of the band gap E_g on the index l_1 for each type of edge-modified ZGNRs (see Figs. 7, 8). Figure 7 shows the dependences for A60 nanoribbons of the series $3n = 1$ and $3n + 2$. The line E_g, which corresponds to the series $3n$ of A60 nanoribbons, as can be seen from Fig. 5, almost does not change its position. It can be seen from Figs. 7a and 7b that, for different series of A60 nanoribbons, the dependences of the band gap on the length of the GNR arm have opposite characters. In both cases, it is seen that, with an increase in the arm length l_1, these dependences of the band gap E_g tend to a certain limit, which is close to the band gap of the armchair GNRs constituting the edge-modified ZGNR. In the case of

the A60 nanoribbon with $w = 7$, the band gap of the armchair GNR with 14 carbon atoms in the unit cell is equal to 1.3 eV, and the limiting values in the corresponding graph lie in the range of 1.0−1.2 eV (see Fig. 7a). In addition, it should be noted that the most effective control of the band gap by varying the arm length is observed for small indices of the arms $l_1 < 10$. This observation also holds true for other types of edge-modified GNRs shown in Figs. 7 and 8. It can be seen from Fig. 7 for the Z60 nanoribbons that, if we exclude from our consideration the point $l_1 = 1$, the dependence is monotonic: it has no maxima which are present, for example, in the dependence shown in Fig. 7d for the A120 nanoribbons. The position of the maximum in this dependence shifts toward higher values of l_1 with an increase in the parameter l_2, and the edges of the maximum become more gently sloping. Interestingly, the maximum value of the band gap E_g in the dependence for the A120 nanoribbons does not
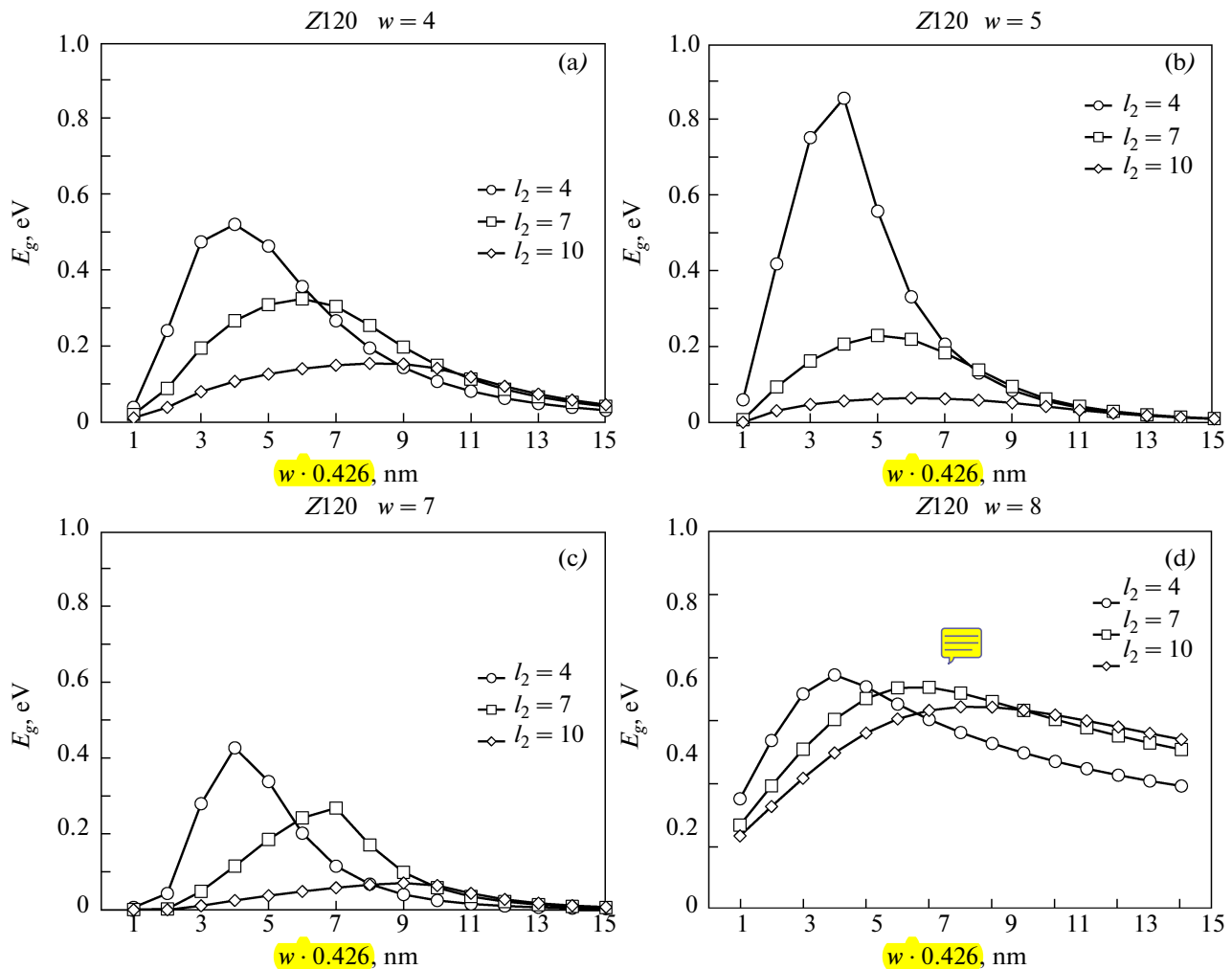
Fig. 8. Dependences of the band gap E_g on the length of the GNR arm l_1 for the nanoribbons Z120 with different widths ($w = 4$, 5, 7, 8).

decrease with an increase in the length of the arm (see Fig. 7d), which is the case for other edge-modified ZGNRs. For the same width of the A120 nanoribbons with equal lengths of the arms, the band gap is larger than that for the nanoribbons with different lengths of the arms.

Despite the fact that, for the Z120 nanoribbons, as well as for the A60 nanoribbons, there are oscillations of the band gap as a function of w (see Fig. 6), we should note that, within this type of edge-modified ZGNRs, the series $3n$, $3n + 1$, and $3n + 2$ are distinguished only conditionally. The point is that, while the series for the A60 nanoribbons can be defined as a sequence of minima, maxima, and intermediate values in oscillations of the band gap, in the case of the Z120 nanoribbons this cannot be done. It can be seen from Figs. 6a and 6b that the series of minimum values for some of the arm length can become the series of intermediate values for other arm lengths. This behavior is observed in Fig. 8. The change in the band gap

due to variations in the arm index l_1 for nanoribbons with a large index of the width can be larger (see Fig. 8, $l_2 = 4$) and smaller (in Fig. 8, $l_2 = 7$) than those for the nanoribbons with a lower index. As a result, the maxima in Figs. 8a and 8c for $l_2 = 4$ are smaller than the corresponding maxima of the band gap E_g in Figs. 8b and 8d. The jumps of the band gap E_g can reach 0.3 eV, which, in the order of magnitude, are comparable with the jumps caused by variations in the width of the edge-modified ZGNRs. However, this is rather the exception than the rule and is characteristic of only the Z120 nanoribbons. In contrast to the series $3n + 2$ (see Figs. 8b, 8d), the series $3n + 1$ (see Figs. 8a, 8c) is characterized not only by a decrease in the absolute value of the maximum of the band gap E_g, but also by a larger shift of this maximum toward higher values of l_1 with an increase in the length l_2 of the GNR arm.

The presented values of the band gap of the edge-modified ZGNRs correspond to radiative electronic

transitions occurring in the infrared frequency range ($E_g < 1$ eV). Thus, the field of application of materials containing edge-modified ZGNRs can be the region of functional nanomaterials for the infrared spectral range, which can be used in the fabrication of detectors, emitting devices, protective coatings, etc.

6. CONCLUSIONS

In this work, we have proposed that the band gap of graphene nanoribbons can be controlled by varying two new parameters of the periodic edge-modified zigzag GNR, namely, two GNR arms. We considered a class of graphene nanoribbons that are asymmetric with respect to the nanoribbon axis due to the edge-modified ZGNR structure. For these structures, we proposed a classification of edge-modified ZGNRs and a method for the description of their geometry, which is similar to the description of CNTs. It is important to emphasize that this description takes into account the asymmetry associated with different lengths of the GNR arms. This circumstance can be extended to other classes of graphene structures, for example, graphene nanowigglers, for which methods of synthesis already exist and are rapidly developing [13, 38]. It is quite probable that these methods can also be used for the synthesis of edge-modified ZGNRs. Using the developed classification of edge-modified ZGNRs and method for the description of their structures, we investigated the dependence of the band gap on the nanoribbon length and GNR arm in terms of the π-electron tight-binding method taking into account possible deformations of carbon bonds. It was shown that the band gap decreases exponentially with increasing width of the Z60 nanoribbons. The dependence of the band gap on the width of the nanoribbons Z120 and A60 exhibits oscillations. It was demonstrated that the band gap of the structure can be smoothly changed by varying the GNR arm. This can be used in optical nanodevices operating in the infrared frequency range. It is of interest that, even for structures of the same type, the GNR arm can differently affect the band gap of the edge-modified ZGNR, as is the case for different series of A60 nanoribbons. The results obtained in this study provide a basis for the investigation of electromagnetic and transport properties of objects of this type. Moreover, they can find use in graphene-based nanoelectronics when creating active elements and their junctions.

ACKNOWLEDGMENTS

REFERENCES

1. P. B. Sorokin and L. A. Chernozatonskii, Phys.—Usp. **56** (2), 105 (2013).
2. M. Fujita, K. Wakabayashi, K. Nakada, and K. Kusakabe, J. Phys. Soc. J. **65**, 1920 (1996).
3. K. S. Novoselov, A. K. Geim, S. V. Morozov, D. Jiang, Y. Zhang, S. V. Dubonos, I. V. Grigorieva, and A. A. Firsov, Science (Washington) **306**, 666 (2004).
4. V. Barone, O. Hod, and G. E. Scuseria, Nano Lett. **6**, 2748 (2006).
5. M. Ezawa, Phys. Rev. B: Condens. Matter **73**, 045432 (2006).
6. D. A. Areshkin, D. Gunlycke, and C. T. White, Nano Lett. **7**, 204 (2007).
7. C. T. White, J. Li, D. Gunlycke, and J. W. Mintmire, Nano Lett. **7**, 825 (2007).
8. D. Gunlycke and C. White, Phys. Rev. B: Condens. Matter **77**, 115116 (2008).
9. K. A. Ritter and J. W. Lyding, Nat. Mater. **8**, 235 (2009).
10. M. Han, B. Ozyilmaz, Y. Zhang, and P. Kim, Phys. Rev. Lett. **98**, 206805 (2007).
11. M. Koch, F. Ample, C. Joachim, and L. Grill, Nat. Nanotechnol. **7**, 713 (2012).
12. L. Jiao, L. Zhang, X. Wang, G. Diankov, and H. Dai, Nature (London) **458**, 877 (2009).
13. J. Cai, P. Ruffieux, R. Jaafar, M. Bieri, T. Braun, S. Blankenburg, M. Muoth, A. P. Seitsonen, M. Saleh, X. Feng, K. Mullen, and R. Fasel, Nature (London) **466**, 470 (2010).
14. W. Li and R. Tao, J. Phys. Soc. Jpn. **81**, 024704 (2012).
15. W. J. Yu and X. Duan, Sci. Rep. **3**, 1248 (2013).
16. S. Bhattacharya and S. Mahapatra, Physica E (Amsterdam) **44**, 1127 (2012).
17. X. Zhong, R. Pandey, and S. P. Karna, Carbon **50**, 784 (2012).
18. Y. C. Huang, C. P. Chang, and M. F. Lin, J. Appl. Phys. **104**, 103314 (2008).
19. M. Topsakal, V. M. K. Bagci, and S. Ciraci, Phys. Rev. B: Condens. Matter **81**, 205437 (2010).
20. W. Jaskolski, A. Ayuela, M. Pelc, H. Santos, and L. Chico, Phys. Rev. B: Condens. Matter **83**, 235424 (2011).
21. Z. F. Wang, Q. W. Shi, Q. Li, X. Wang, J. G. Hou, H. Zheng, Y. Yao, and J. Chen, Appl. Phys. Lett. **91**, 053109 (2007).
22. H. Sevincli, M. Topsakal, and S. Ciraci, Phys. Rev. B: Condens. Matter **78**, 245402 (2008).
23. M. Topsakal, H. Sevincli, and S. Ciraci, Appl. Phys. Lett. **92**, 173118 (2008).
24. S. Ihnatsenka, I. Zozoulenko, and G. Kirczenow, Phys. Rev. B: Condens. Matter **80**, 155415 (2009).
25. L. A. Chernozatonskii, P. B. Sorokin, and J. W. Brüning, Appl. Phys. Lett. **91**, 183103 (2007).
26. A. K. Singh and B. I. Yakobson, Nano Lett. **9**, 1540 (2009).

27. L. A. Chernozatonskii and, P. B. Sorokin, J. Phys. Chem. C **114**, 3225 (2010).

28. E. Costa Girão, L. Liang, E. Cruz-Silva, A. G. S. Filho, and V. Meunier, Phys. Rev. Lett. **107**, 135501 (2011).

29. E.C. Girão, E. Cruz-Silva, and V. Meunier, ACS Nano **6**, 6483 (2012).

30. R. Saito, G. Dresselhaus, and M. Dresselhaus, *Physical Properties of Carbon Nanotubes* (Imperial College Press, London, 1998), p. 276.

31. B. Partoens and F. Peeters, Phys. Rev. B: Condens. Matter **74**, 075404 (2006).

32. R. M. Ribeiro, V. M. Pereira, N. M. R. Peres, P. R. Briddon, and A. H. Castro Neto, New J. Phys. **11**, 115002 (2009).

33. R. Saito, M. Fujita, G. Dresselhaus, and M. Dresselhaus, Phys. Rev. B: Condens. Matter **46**, 1804 (1992).

34. S. Plimpton, J. Comput. Phys. **117**, 1 (1995).

35. S. J. Stuart, A. B. Tutein, and J. A. Harrison, J. Chem. Phys. **112**, 6472 (2000).

36. Y.-W. Son, M. L. Cohen, and S. G. Louie, Phys. Rev. Lett. **97**, 216803 (2006).

37. A. Akhmerov and C. Beenakker, Phys. Rev. B: Condens. Matter **77**, 085423 (2008).

38. T. H. Vo, M. Shekhirev, D. A. Kunkel, M. D. Morton, E. Berglund, L. Kong, P. M. Wilson, P. A. Dowben, A. Enders, and A. Sinitskii, Nat. Commun. **5**, 1 (2014).

Translated by O. Borovik-Romanova

SPELL: OK